Proceedings of 10th International Conference on Precision, Meso, Micro and Nano Engineering (COPEN 10)
December 07 – 09, 2017, Indian Institute of Technology Madras, Chennai – 600 036 INDIA

Vibration Attenuation in Boring Operation using Fiber Reinforced Composites

B.A.G.Yuvaraju* and B.K.Nanda

Production Engineering Section, Department of Mechanical Engineering
National Institute of Technology, Rourkela - 769 0086, INDIA

Abstract

Unwanted vibration in machine tools like lathe, milling, grinding and other machine tools is one of the elementary problems as it affects the quality of the machined parts, tool life, and noise during machining operations. Particularly, in boring operation, the vibrations induced are the primary concern in the manufacturing industries. Hence, these unwanted vibrations are desired to be suppressed or damped out while machining. In present work, the damping ratios and natural frequencies of the boring bar vibrations have been estimated during boring operation with different composites such as Glass Fiber Reinforced Polyester (GFRP) and Glass Fiber Reinforced Epoxy (GFRE) on the tool post. It has been observed that GFRE composite gives good results compared to other composites. Further, the Fast Fourier Transform (FFT) technique has been utilized to find out the values of spectral power density and magnitude for various combinations of composites.

Keywords: Damping, Damping ratio, Natural Frequency, Composite.

1. INTRODUCTION

Present manufacturing industries are facing challenges in producing more accurate and precise products as there is a lot of vibrations generated by the cutting tool during the machining operation. Boring is one such machining operation in which pre-drilled holes are enlarged. Usually, the boring bar is the weakest section of the tool clamping system in the lathe machine. The movement of the boring bar may vary with time. A long and slender boring bar is more sensitive to the excitation brought in by the material deformation which is caused by the machining process. Dynamic motion, i.e. vibration is the result of workpiece deformation. This vibration affects the surface finish of the workpiece as well as tool life during the boring process. The work surface produced should be better surface finish, since boring is semi finishing operation. Hence, the induced vibrations must be suppressed to improve the machined surface. These vibrations in the machine tool are depreciated by using the passive dampers.

Bert and Nashif [1, 2] have investigated the fiber reinforced composites to minimise the vibration, and they found that fiber reinforced composites exhibit more damping compared to metallic structural materials. Lazan [3] has extensively studied the material damping and concluded that the dynamic stresses are directly related to logarithmic decrement value. Haranath et al. [4] analyzed the machine tool structures dynamically and observed enhanced damping parameters. Rivin et al. [5] have worked on the boring bar with large slenderness ratio and found the redesigned tool with viscoelastic layers has improved stability, stiffness and damping. Ema et al. [6] studied the effect of shear deformation on natural frequency in the transverse direction as well as loss factor using finite element analysis and observed an improvement in damping capacity of the boring bar with the use of impact dampers. Rahman et al. [7] used several materials to study the damping in machine tools and noted that composite materials have an excellent stiffness. Hence it is a better replacement for the cast iron to get the improved surface finish of the product.

Various techniques are used to measure a material damping properties, but the accurate estimation of these parameters is complicated. These are used to formulate an analytical model describing the input-output relationship of the system. The standard method of measuring system's response is by Fourier analysis. Nagarajaiah [8] developed time frequency algorithms to identify these parameters and control a multi degree freedom system (MDOF) response with smart tuned mass dampers (STMD) using short time Fourier transforms. However, it is not possible to study the time varying characteristics of the signal in Fourier transform. Because of this, Newland [9] developed wavelet transform technique as a signal processing tool for estimating the damping properties. Chui [10] used long and short windows at low and high frequencies respectively. This decomposition assists in monitoring discontinuities and transient behavior of signals. Kijewski et al. [11] and Slavic et al. [12] have adopted various techniques of improvement of parameters using Morlet wavelet transform. Dziedziech et al. [13] presented a method to estimate damping, natural frequency and mode shapes utilizing signal post processing and random input excitation based on Crazy Climbers algorithm. Sahekhaini et al. [14] suggested an algorithm for modal parameter estimation and damage detection using complex Morlet wavelet and natural frequencies of the system are identified by using wavelet transform. All these studies authenticate that wavelet transform is an advanced technique for signal processing compared to other methods

In this paper, GFRE and GFRP composites are used as passive dampers and placed under the boring bar to reduce the vibrations induced during boring operation. The damping parameters such as damping ratios and natural frequencies are estimated using experimental and validated by wavelet transform method.

2. WAVELET TRANSFORM METHOD

A single-degree of freedom system is utilized for stability analysis of the cutting process in boring operation. Either the workpiece or tool being weak in stiffness in the orthogonal direction is considered. We assumed the system as the single degree of freedom (s-dof) self-excited linear time-invariant vibration system since the boring bar is the weakest member in the tool clamping system. Consider a body of mass *m* is connected to a spring and viscous damper to a fixed support,

*B.A.G. Yuvaraju, Email: bagyuvaraju@gmail.com

ISBN: 978-93-80689-28-9

which produces self-excited vibrations, the equation of motion of the body is expressed as:

$$m\ddot{x} + c\dot{x} + kx = 0 \quad (1)$$

where x is the displacement of a mass m, c and k are the damping coefficient and stiffness respectively.

The Eq. (1) is expressed in terms of natural frequency ω_n and damping ratio ζ as:

$$\ddot{x} + 2\zeta\omega_n\dot{x} + \omega_n^2 x = 0 \quad (2)$$

where $\omega_n^2 = \frac{k}{m}$ and $\zeta = \frac{c}{2\sqrt{mk}}$. It is assumed that $0 < \zeta < 1$.

The solution of the above equation is expressed by:

$$x(t) = x_0 e^{-\zeta\omega_n t}\cos(\omega_d t - \alpha) \quad (3)$$

where x_0 and α depend on initial boundary condition, and $\omega_d = \omega_n\sqrt{1-\zeta^2}$ is the damped natural frequency.

The Morlet wavelet in time domain can be defined as:

$$\psi(t) = e^{-\frac{t^2}{2\sigma^2}}\left(e^{i\omega_o t} - e^{-\frac{\omega_o^2}{2}}\right) \quad (4)$$

where, ω_0 is central frequency and σ is bandwidth parameter.

Eq. (4) must satisfy the following conditions:

$$\int_{-\infty}^{\infty}|\psi(t)|^2 dt < \infty \quad (5)$$

$$c_\psi = 2\pi\int_{-\infty}^{\infty}\frac{|\Psi(\omega)|^2 d\omega}{|\omega|} < \infty \quad (6)$$

The Morlet wavelet transform can be expressed as:

$$W(a,b) = \frac{1}{\sqrt{a}}\int_{-\infty}^{\infty} x(t)\psi'\left(\frac{t-b}{a}\right)dt \quad (7)$$

where, $x(t)$ is original signal and ψ' is complex conjugate of mother wavelet.

By setting $\tau = \left(\frac{t-b}{a}\right)$, the wavelet transform of the system response defined in Eq. (7) is transformed to:

$$W(a,b) = \sqrt{a}\int_{-\infty}^{\infty} x(a\tau + b)\psi'(\tau)d\tau \quad (8)$$

Substituting Eq. (4) in Eq. (8) and the cosine function is expressed as an exponential function, we obtain

$$W(a,b) = \frac{1}{2}x_0\sqrt{a}e^{-\zeta\omega_n b}\left[I_1 + I_2 - I_3 - I_4\right] \quad (9)$$

where, $I_1 = \int_{-\infty}^{\infty} e^{-\frac{\tau^2}{2} - (i\omega_o + \zeta\omega_n a - i\omega_d a)\tau + i(\omega_d b - \alpha)}d\tau$ (10)

$$I_2 = \int_{-\infty}^{\infty} e^{-\frac{\tau^2}{2} - (i\omega_o + \zeta\omega_n a + i\omega_d a)\tau - i(\omega_d b - \alpha)}d\tau \quad (11)$$

$$I_3 = \int_{-\infty}^{\infty} e^{-\frac{\tau^2}{2} - (\zeta\omega_n a - i\omega_d a)\tau + i(\omega_d b - \alpha) - \frac{\omega_o^2}{2}}d\tau \quad (12)$$

$$I_4 = \int_{-\infty}^{\infty} e^{-\frac{\tau^2}{2} - (\zeta\omega_n a + i\omega_d a)\tau + i(\omega_d b - \alpha) - \frac{\omega_o^2}{2}}d\tau \quad (13)$$

substituting the solutions of Eqs. (10) to (13) in Eq. (9), we obtain

$$W(a,b) = \frac{1}{2}x_0\sqrt{2\pi a}e^{-\zeta\omega_n b - \frac{1}{2}\left[\left(1-2\zeta^2\right)\omega_n^2 a^2 + \omega_o^2\right]}\left[e^{\theta} + e^{-\theta} - e^{\theta'} - e^{-\theta'}\right] \quad (14)$$

where, $\theta = \left(i\zeta\omega_o\omega_n a - i\zeta\omega_n\omega_d a^2 + \omega_o\omega_d a\right) + i\left(\omega_d b - \alpha\right)$ and $\theta' = \left(-i\zeta\omega_n\omega_d a^2\right) + i\left(\omega_d b - \alpha\right)$

Since $\left|e^{\theta}\right| >> \left|e^{-\theta}\right|$ and $\left|e^{\theta'}\right| >> \left|e^{-\theta'}\right|$, therefore Eq. (14) reduces to:

$$W(a,b) = \frac{1}{2}x_0\sqrt{2\pi a}e^{-\zeta\omega_n b - \frac{1}{2}\left[\left(1-2\zeta^2\right)\omega_n^2 a^2 + \omega_o^2\right]}e^{\theta}\left[1 - e^{-i\zeta\omega_o\omega_d a - \omega_o\omega_d a}\right] \quad (15)$$

Since the value of $\omega_o >> 1$, the value $e^{-i\zeta\omega_o\omega_d a - \omega_o\omega_d a}$ becomes very small and Eq. (15) is modified as:

$$W(a,b) \approx \frac{1}{2}x_0\sqrt{2\pi a}e^{A+iB} \quad (16)$$

where $A = -\zeta\omega_n b - \frac{1}{2}\left(\left(1-2\zeta^2\right)\omega_n^2 a^2 + \omega_o^2\right) + \omega_o\omega_d a$, and $B = \left[-\zeta\omega_n\omega_d a^2 + \zeta\omega_o\omega_n a + \left(\omega_d b - \alpha\right)\right]$

By fixing the scaling factor $a = a_0$ and varying translation *b*, we obtain

$$\ln\left|W(a_0,b)\right| \approx -\zeta\omega_n b + c_1 \quad (17)$$

$$\angle W(a_0,b) \approx \omega_d b + c_2 \quad (18)$$

where c_1 and c_2 are independent of the translation, *b*, and are given by:

$$c_1 = -\frac{1}{2}\left[\left(1-2\zeta^2\right)\omega_n^2 a_0^2 - 2\omega_o\omega_d a_0 + \omega_o^2\right] + \ln\frac{\sqrt{2\pi a_0}x_0}{2}$$ and

$$c_2 = -\zeta\omega_n\omega_d a^2 + \zeta\omega_o\omega_n a - \alpha$$

Now it is evident that the damping ratio ζ and natural frequency ω_n can be estimated from Eqs. 17 and 18.

Slope of $\ln\left|W(a_0,b)\right|$ Vs. $\tau = -\zeta\omega_n$ and (19)

Slope of $\angle W(a_0,b)$ Vs. $b = \omega_n\sqrt{1-\zeta^2}$ (20)

Eqs. (19) and (20) hold good for any fixed *a* and any range of *b*. In general, it is noted that the free response of the system given in Eq. (3) is valid only for a positive time, and $x(t) = 0$, $\forall t < 0$. Further, it is observed that the wavelet transform works as a window in time and frequency domains for given *a* and *b*. Thus, the derivation is not authentic if *b* being too small. Usually, the output signal is contaminated with noise, which affects the results. Hence, the wavelet transform of a practical response is given by:

$$\tilde{W}(a,b) = W(a,b) + W_n(a,b) \quad (21)$$

where $\tilde{W}(a,b)$ represents the practical response and $W_n(a,b)$ is the noise. Proper selection of a_o and *b* values will give better results to satisfy the following condition.

$$\left|W_n(a_0,b)\right| << \left|W(a_0,b)\right| \quad (22)$$

This indicates that the contribution from noise is negligible.

Hence, the mother wavelet and Morlet wavelet transform chosen in Eq.s (4) and (7) respectively are suitable for the analysis of boring bar undergoing vibrations.

3. EXPERIMETNAL DETAILS

3.1 Setup and Procedure

The experimental setup mainly consists of a conventional lathe, boring bar with inserts, and workpiece of mild steel, composite plates, contact type accelerometer and digital storage oscilloscope. Figures 1 and 2 show the geometry of the cutting insert and schematic diagram of the experimental setup. Table 1 represents the dimensions of the cutting tool insert.

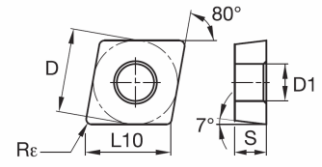

Fig. 1: Geometry of the cutting insert

Table 1: Dimensions of the insert shown in geometry

Insert type	D	L10	S	R_ε	D1
CCMT09T308-MU TN2000	9.53	9.67	3.97	0.8	4.40

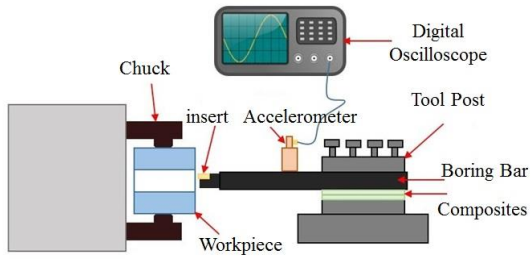

Fig. 2: Schematic diagram of experimental setup

A carbide insert is fixed to the boring bar and mounted on tool post of the lathe. Now, a workpiece of mild steel is held in the chuck. An accelerometer is connected to the boring bar in the cutting speed direction to measure the vibrations during machining. These signals are fed to the oscilloscope from the accelerometer for recording and further analysis. The RMS value of the signals, damping ratio and natural frequency are estimated using the recorded data. The experiments are repeated by placing different composites, i.e. Glass Fiber Reinforced Epoxy (GFRE) and Glass Fiber Reinforced Polyester (GFRP) under the tool. Further, the surface roughness of the machined part is measured using Taylor Hobson Talysurf tester. Then after, readings are attained at three locations along the workpiece length, and the average of them is determined. The machining parameters of various level used in boring operation are given in Table 2. Cutting speed and feed determines the surface finish, power requirements, and material removal rate. The primary factor in choosing feed and speed is the material to be cut. However, one should also consider material of the tool, rigidity of the workpiece, size and condition of the lathe, and depth of cut. Here the workpiece material is mild steel and tool of carbide insert. Since boring is the finishing operation the surface finish produced to be more accurate and hence the speed and feed should be as low as possible. The temperature developed during machining will be more if the speed and feed are more and result in poor surface finish. The optimum speed to bore a diameter of 30 mm is in between 90 rpm and 250 rpm and feed is about 0.1 to 0.3 mm/rev. Hence we selected the parameters as shown in Table 2.

Table 2: Machining Parameters Used in Boring Operation

Process Parameter	Level-1	Level-2	Level-3
Speed (rpm)	92	140	220
Feed (mm/rev)	0.1	0.2	0.3
Depth of cut (mm)	0.1	0.2	0.3

3.2 Design Matrix

A three-factor three-level Box-Behnken design (BBD) with three center points and a single block is generated from the design of experiments. Table-3 represents the experimental results of vibration amplitude and surface roughness.

3.3 Estimation of Damping Parameters

The damping in the domain of time is estimated by using logarithmic decrement method. The displacement of vibration amplitude of the system is measured and recorded in this method. Figure 3 shows logarithmic decrement plot. Logarithmic decrement is defined as the natural logarithmic of the ratio of any two successive peak amplitudes.

Logarithmic decrement is used to determine the damping ratio of an underdamped system in the time domain, which is given below:

$$\delta = \frac{1}{n}\ln\left(\frac{x(t)}{x(t+nt)}\right) \tag{23}$$

where $x(t)$ is amplitude at time t and $x(t+nt)$ is the amplitude of peak n period, where n is any integer number of successive, positive peaks.

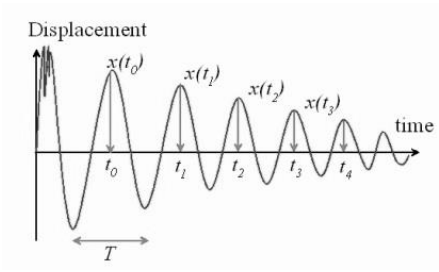

Fig. 3: Logarithmic decrement plot

Thus, the damping ratio is determined from logarithmic decrement using the expression given below:

$$\zeta = \frac{1}{\sqrt{1+\left(\frac{2\pi}{\delta}\right)^2}} \tag{24}$$

Further, the value of damping ratio is used to find the natural frequency ω_n of the system from damped natural frequency ω_d :

$$\omega_d = \frac{2\pi}{T} \tag{25}$$

$$\omega_n = \frac{\omega_d}{\sqrt{\left(1-\zeta^2\right)}} \tag{26}$$

Table 3: Experimental Results of Vibration Amplitude and Surface Roughness

Machining Parameters			No Composite		GFRP		GFRE	
v	f	d	A	Ra	A	Ra	A	Ra
140	0.1	0.1	140.64	6.1	133.51	5.54	89.85	5.13
220	0.3	0.2	252.63	12.5	227.15	12.07	167.18	11.13
220	0.2	0.1	206.89	11.02	234.85	9.03	166.5	7.87
140	0.3	0.1	144.18	11.83	144.95	10.03	122.16	8.67
220	0.1	0.2	199.13	8.93	334.86	5.03	211.74	5.1
92	0.1	0.2	121.74	5.83	162.8	8.57	47.06	7.6
92	0.2	0.1	109.14	10.03	71.71	7.83	59.17	8.87
140	0.2	0.2	238.42	12.47	169.41	12.2	128.61	11.47
140	0.1	0.3	241.07	12.03	236.22	9.03	176.95	7.6
140	0.3	0.3	243.85	13.67	180.61	11.87	153.2	11.47
220	0.2	0.3	239.94	14.1	248.04	11.47	277.65	10.2
140	0.2	0.2	239.99	13.03	176.75	10.87	140.06	9.33
140	0.2	0.2	265.54	11.8	176.75	9.2	120.95	10.8
92	0.3	0.2	156.98	13.01	129.95	11.27	101.57	11.2
92	0.2	0.3	190.012	12.33	129.92	11.93	86.01	9.17

v-speed, rpm; f-feed, mm/rev; d-depth of cut, mm; A-amplitude; Ra-Surface roughness;
GFRP-Glass Fiber Reinforced Polyester; GFRE-Glass Fiber Reinforced Epoxy;

where *T is* the period of the waveform, which is given by the time elapsed between two adjacent peaks of amplitudes for under damped system.

The logarithmic decrement method becomes less and less precise as the damping ratio increases past above 0.5. This method is not applied to a system which is having the damping ratio greater than 1.0 since the system is over damped.

4. RESULTS AND DISCUSSIONS

The damping parameters of boring bar vibrations using various composites such as GFRE, GFRP are estimated experimentally and are validated using wavelet transform method. The results obtained by the wavelet transform method are given below.

4.1 Estimation of Damping Parameters Using Wavelet Transform Method

The Morlet wavelet transform of single degree of freedom linear vibrations with central frequency, ω_0 at 10 rad/s is shown in Figure 4 which clearly indicates that there is a maximum peak of scaling parameters at 40 sec.

The corresponding logarithmic modulus and phase are plotted with translation parameter as shown in Figures 5 and 6 respectively for GFRE composite. It is observed that there exists a linear relationship between the plots, i.e. logarithmic modulus vs. translation parameter and phase vs. translation parameter for a smaller range of positive values i.e., 0 and 5. The slopes of logarithmic modulus and phase plots are obtained with the help of interpolate method using curve fitting software. Then, damping ratios and natural frequencies are estimated using Eqs. (19) and (20).

From table 4, it is noticed that the damping ratios are increased with the use of GFRE compared to GFRP and without composite. This is mainly due to GFRE is more viscoelastic in nature compared to GFRP. Hence, GFRE composites dissipate more energy compared to GFRP. Similarly, the natural frequencies are decreased with the use of GFRE compared to GFRP and without composite. The values of damping ratios and natural frequencies obtained from the experimental as well as wavelet analysis are presented in Table-4 for different composites. Also the percentage errors are calculated and observed that the error in damping ratios and natural frequencies are less than 4% and 1% respectively, which is reasonable. Particularly in case of without composites the negative error in natural frequency represents the harmonic motion of the tool vibration in negative direction.

Table 4: Results from both experimental and wavelet analyses

Type of composite	ζ	ζ'	Error in ζ' (%)	ω_n (rad/s)	ω_n' (rad/s)	Error in ω_n' (%)
Without Composite	0.00039	0.000397	1.898409	64.1534	64.15	-0.00530
GFRP	0.0012	0.001238	3.166667	64.8086	64.81	0.00216
GFRE	0.0018	0.001831	1.722222	63.9056	63.9101	0.00704

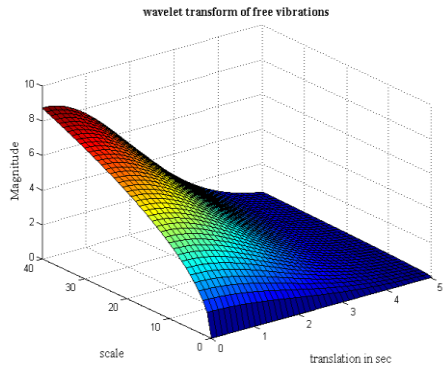

Fig. 4: Morlet Wavelet Transform of boring bar vibrations composite

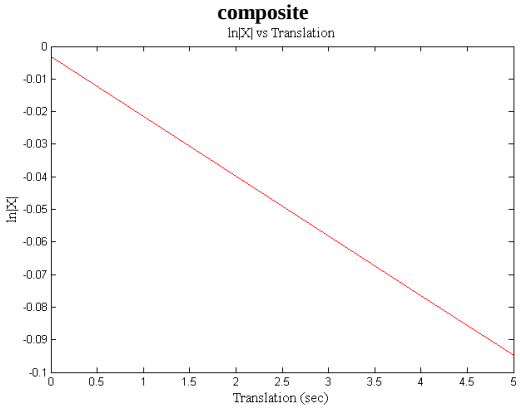

Fig. 5: Logarthemic modulus Vs translation plot for GFRE

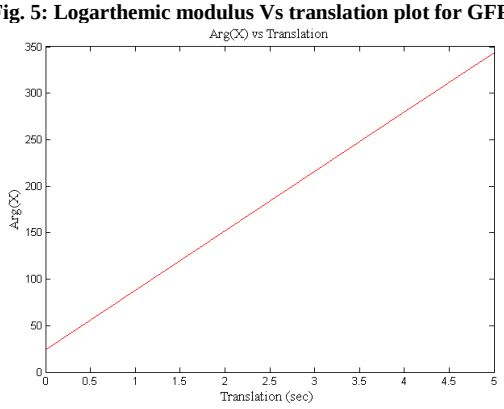

Fig. 6: Phase vs translation plot for GFRE composite

From Table-4, it is noticed that the damping ratio is more in case of GFRE composite compared to other conditions. Thus, GFRE composites are best suitable dampers given in present paper to suppress the vibrations.

The Fast Fourier Transform is employed to find out the spectral power density and magnitude spectrum from the recorded signals during experimentation. Fig. 7 shows the FFT of the vibration signal for GFRE composite at optimal parameter setting. The results of FFT for various composites are presented in Table 5 and observed that the value of spectral power density and magnitude spectrum are very small for GFRE composites compared to other.

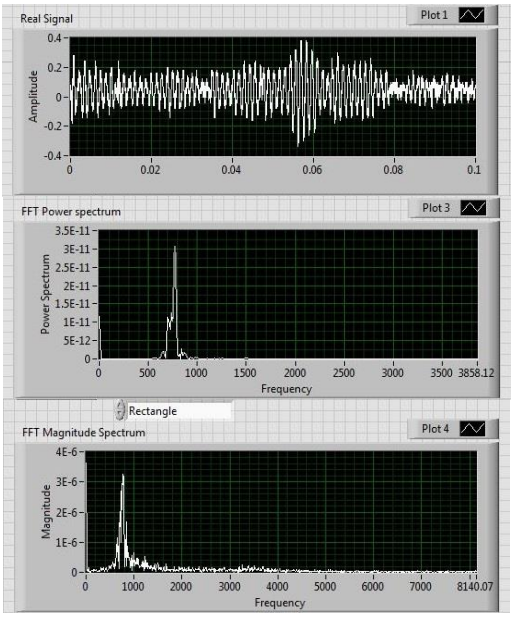

Fig. 7: FFT of recorded signal for GFRE composite

Table 4: Results from Fast Fourier Transform

Type of Composite	FFT	
	Spectral Power Density (W/Hz)	Magnitude of Amplitude (mV)
Without composite	8.87×10^{-11}	6.65×10^{-6}
GFRP	6×10^{-11}	6.52×10^{-6}
GFRE	3.23×10^{-11}	3.42×10^{-6}

5. CONCLUSIONS

The wavelet transform method has been employed to identify and calculate the damping ratio and natural frequency for different composites. From the analysis, it has been determined that the validation of the relationship between wavelet and experimental results depend on the translation, scaling and the central frequency of the Morlet wavelet. Therefore, the accuracy of parameter identification depends on a, b and ω_0 .

Numerical simulations show that the errors obtained for damping ratio and natural frequency are less than 4% and 1% respectively for the boring bar with various composites. Since the percentage error of damping ratios and natural frequencies are very small, the results are reasonable and the analysis is authentic.

Further, the Fast Fourier Transform is applied to find out the spectral power density and magnitude from recorded signals during experimentation. It has been observed that GFRE composite gives better results compared to other composites. The values obtained from the FFT magnitude and spectral power densities are 3.42x10-6 mV and 3.23x10-11 W/Hz respectively for GFRE composite.

References

[1] C.W. Bert, "Composite materials: A survey or the damping capacity of fiber reinforced composites in damping applications for vibration control," Oklahoma Univ Norman School of Aerospace Mechanical And Nuclear Engineering, 1980.

[2] A.D. Nashif, D.I. Jones, and J.P. Henderson, "Vibration Damping," *A wiley inter-science publication*, 1985.

[3] B.J. Lazan, "Damping of materials and members in structural mechanics," *Pergamon Press Ltd, Oxford, England*, 1968.

[4] S. Haranath, N. Ganesan, and B.V.A. Rao, "Dynamic analysis of machine tool structureswith applied damping treatment," *Int. J. Mach. Tools Manuf.*, **27(1):** 43–55, 1987.

[5] E.I. Rivin, and H. Kang, "Improvement of machining conditions for slender parts by tuned dynamic stiffness of tool," *Int. J. Mach. Tools Manuf.*, **29(3):** 361–376, 1989.

[6] S. Ema, E. Marui, "Suppression of chatter vibration of boring tools using impact dampers," *Int. J. Mach. Tools Manuf.*, **40(8):**1141–1156, 2000.

[7] M. Rahman, A. Mansur, and B. Karim, "Non-conventional Materials for Machine Tool Structures," *JSME Int. J. Ser. C Mech. Syst. Mach. Elem. Manuf.*, **44(1):**1–11, 2001.

[8] Nagarajaiah S, "Adaptive passive, semi active, smart tuned mass dampers: identification and control using empirical mode decomposition, Hilbert transform, and short-term Fourier transform," *Structural Control and Health Monitoring*, **16(7-8):** 800-841, 2009.

[9] Newland DE, "Wavelet analysis of vibration, Part 1: Theory," *Journal of vibration and acoustics*, **116(4**): 409-416, 1994.

[10] Chui CK (1992), "An introduction to wavelets," New York: Academic Press, 1992.

[11] Kijewski T, Kareem A, "On the presence of end effects and their melioration in wavelet-based analysis," *Journal of Sound and Vibration*, **256(5**): 980-988, 2002.

[12] Slavic J, Simonovski I, Boltezar M, "Damping identification using a continuous wavelet transform: application to real data," *Journal of Sound and Vibration*, **262(2):** 291-307, 2003.

[13] Dziedziech K, Staszewski W, and Uhl, "Wavelet-based modal analysis for time-variant systems," *Mechanical Systems and Signal Processing*, **50**: 323-337, 2015.

[14] Sahekhaini A, Muhamad P, Kohiyama M, et al., "A Study on Structural System Identification and Damage Detection for Free Vibration Response Using the Wavelet Transform," *Applied Mechanics and Materials*, **752**: 1029-1034, 2015.